Microtubules Are Stabilized in Confluent Epithelial Cells But Not in Fibroblasts

Rainer Pepperkok, Marie Hélène Bré, Jean Davoust, and Thomas E. Kreis

European Molecular Biology Laboratory, 6900 Heidelberg, Federal Republic of Germany

Abstract. Rhodamine-tagged tubulin was microinjected into epithelial cells (MDCK) and fibroblasts (Vero) to characterize the dynamic properties of labeled microtubules in sparse and confluent cells. Fringe pattern fluorescence photobleaching revealed two components with distinct dynamic properties. About one-third of the injected tubulin diffused rapidly in the cytoplasm with a diffusion coefficient of 1.3–1.6 $\times 10^{-8}$ cm^2/s. This pool of soluble cytoplasmic tubulin was increased to >80% when cells were treated with nocodazole, or reduced to ~20% upon treatment of cells with taxol. Fluorescence recovery of the remaining two-thirds of labeled tubulin occurred with an average half-time ($t_{1/2}$) of 9–11 min. This pool corresponds to labeled tubulin associated with microtubules, since it was sensitive to treatment of cells with nocodazole and since taxol increased its average $t_{1/2}$ to >22 min. Movement of photobleached microtubules in the cytoplasm with rates of several micrometers per minute was shown using very small interfringe distances. A significant change in the dynamic properties of microtubules occurred when MDCK cells reached confluency. On a cell average, microtubule half-life was increased about twofold to ~16 min. In fact, two populations of cells were detected with respect to their microtubule turnover rates, one with a $t_{1/2}$ of ~9 min and one with a $t_{1/2}$ of >25 min. Correspondingly, the rate of incorporation of microinjected tubulin into interphase microtubules was reduced about twofold in confluent MDCK cells. In contrast to the MDCK cells, no difference in microtubule dynamics was observed in sparse and confluent populations of Vero fibroblasts, where the average microtubule half-life was ~10 min. Thus, microtubules are significantly stabilized in epithelial but not fibroblastic cells grown to confluency.

THE microtubules in interphase cells build up a dynamic cytoskeletal network (for a review see Kirschner and Mitchison, 1986) which is essential for the polarized spatial arrangement of cytoplasmic organelles (for a review see Kreis, 1990) and for intracellular membrane traffic (for reviews see Schliwa, 1984; Vale, 1987). An optimal organization of the cytoplasm by microtubules needs both tight control and flexibility towards changes in the cellular environment. Changes in the dynamic properties of microtubules may contribute to alterations of this organization. Reorientation of cells and cell differentiation, for example, clearly have profound effects on the organization and stability of interphase microtubules (Baas et al., 1987; Bacallao et al., 1989; Black and Baas, 1989; Bré et al., 1987; Gundersen et al., 1989; Houliston et al., 1987; Lim et al., 1989) and on the localization of cytoplasmic organelles (Bacallao et al., 1989; Kupfer et al., 1982, 1986; Tassin et al., 1985*a*; Trelstad, 1970). Furthermore, significant alterations in the arrangement of the microtubule organizing material and in microtubule nucleation take place during various forms of cell differentiation (Buendia et al., 1990; Gorbski and Borisy, 1985; Karsenti and Maro, 1986; Morgensen et al., 1989; Tassin et al., 1985*b*; Tucker et al., 1986; see also Bré et al., 1990). The molecular signals which induce alterations in microtubule stability are, so far however, only very poorly understood. Direct assays for microtubule dynamics are needed to characterize these signals.

The dynamic properties of microtubules have been studied in living cells by microinjection of modified microtubule subunits (Keith et al., 1980; Kreis, 1987; Mitchison, 1989; Okabe and Hirokawa, 1988; Olmsted et al., 1989; Sammak et al., 1987; Saxton et al., 1984; Scherson et al., 1984; Schulze and Kirschner, 1986; Soltys and Borisy, 1985). These experiments lead to the conclusion that the half-life of interphase microtubules is on average 5–10 min. Distinct subclasses of microtubules with different dynamic properties have been characterized. Microtubules containing predominantly detyrosinated (Bré et al., 1987; Gundersen et al., 1984; Khawaja et al., 1988; Kreis, 1987; Schulze and Kirschner, 1987; Webster et al., 1987) or acetylated α-tubulin (Black and Keyser, 1987; L'Hernault and Rosenbaum, 1985; Piperno et al., 1987; Webster and Borisy, 1989) appear stabilized. On the other hand, the majority of the mi-

Dr. Bré's present address is Laboratoire de Biologie Cellulaire 4, U.A. CNRS 1134, Université Paris-Sud, 91405 Orsay-Cedex, France. Dr. Davoust's present address is Centre d'Immunology INSERM-CNRS de Marseille-Luminy, Case 906, F-13288 Marseille Cedex 9, France.

totic spindle microtubules are destabilized, relative to the average population of interphase microtubules (for a review see Mitchison, 1988). Stabilizing factors binding to microtubules, microtubule-associated proteins (MAPs),[1] as well as posttranslational modifications of the microtubular components may regulate microtubule stability in vivo (Dinsmore and Sloboda, 1988; Drubin and Kirschner, 1986; Kanai et al., 1989; Lewis et al., 1989; Verde et al., 1990). Interactions of microtubules with other cytoskeletal elements or cytoplasmic structures may also lead to stabilization of subclasses of interphase microtubules.

In this study we have asked whether the dynamic properties of microtubules change when fibroblasts or epithelial cells reach confluency. For this purpose, microtubules have been fluorescently labeled in living cells by microinjection of rhodamine-tagged tubulin (rh-tubulin). Alterations in the average turnover rates of microtubules were measured by fringe pattern fluorescence photobleaching (Davoust et al., 1982; Cosson, Pepperkok, Back, and Davoust, manuscript submitted for publication) in Vero fibroblasts or epithelial MDCK cells grown to different densities. Changes in microtubule nucleation and elongation rates occurring in MDCK cells during the formation of cell–cell contacts are addressed and discussed elsewhere (Bré et al., 1990).

Materials and Methods

Cell Culture and Drug Treatment

MDCK cells, strain II, were grown as described (Bré et al., 1987). For microinjection and fluorescence photobleaching experiments they were seeded on round coverslips (18-mm-diam) at three different densities to give sparse (single cells, or cells growing at the periphery of separate small colonies), confluent (cells forming a monolayer), or highly confluent (cells forming domes in the monolayer, see for example Leighton et al., 1970) cells, respectively, after 2 d of culture. African green monkey kidney cells (Vero cells) were grown as described (Kreis, 1986). Cells were plated to give sparse or confluent cells after 2 d in culture.

Microtubules were depolymerized at 37°C by incubation of Vero cells for 1 h with 10 μM nocodazole and MDCK cells for 4 h with 33 μM nocodazole, respectively (see also Bré et al., 1987). Taxol was used for both cell types at a concentration of 10 μM for 1 h at 37°C.

Microinjection of Rhodamine-labeled Proteins

Microinjection into cells was performed with the automatic microinjection system previously described (Ansorge and Pepperkok, 1988). Cells were incubated for 2 h at 37°C after microinjection, unless otherwise indicated, before photobleaching or immunofluorescence labeling experiments were carried out.

Tubulin from bovine brain was labeled with rhodamine as described elsewhere (rh-tubulin; Kreis, 1987). Rh-tubulin was microinjected at a concentration of 2 mg/ml with a fluorochrome to protein ratio of ~0.2. Rhodamine labeled BSA was prepared as described (Kreis et al., 1982) and microinjected at a concentration of 2 mg/ml.

Fringe Pattern Fluorescence Photobleaching

Fluorescence photobleaching experiments on cells microinjected with fluorescently labeled proteins were performed as described (Davoust et al., 1982; Pollerberg et al., 1986). Briefly, cells microinjected with fluorescently tagged proteins on coverslips were mounted in a Plexiglass chamber containing 400 μl of HBSS supplemented with 0.1% BSA and transferred to the microscope stage (IM 35; Zeiss). The temperature was kept constant at 37°C. A fringe pattern with an interfringe distance of 1.4–20 μm was bleached into the labeled cells by a short pulse (150 msec, 1.5 kW/cm^2, 514 nm) of two coherently interfering laser beams (Argon laser 2020; Spectra-Physics, Inc., Mountain View, CA). ~10% of the cell-associated fluorescence was irreversibly bleached by this flash. Changes in the pattern of contrast were monitored after bleaching by scanning the fringe pattern forth and back (3 kHz) with ~10^4-fold attenuated laser and the intensities of emitted fluorescent light were measured with a photomultiplier (R761-01; Hamamatsu Corp., Tokyo, Japan) coupled to a lock-in amplifier and stored in the computer memory with a time resolution of 300 ms as described. Interfringe distances were adjusted between 1.4 and 20 μm by varying the distance between the two beams in the epifluorescence path of the microscope using a 40× objective (NPL 40× oil, 1.3 NA, Wild/Leitz). Microtubule integrity in photobleached cells was routinely controlled at the end of each photobleaching experiment by either a second photobleaching experiment, direct visualization of the microtubules in the living cells, or immunofluorescence labeling. rh-tubulin fluorescence associated with cells that had been damaged by the microinjection procedure was completely immobile (similar to cells chemically fixed after microinjection and before bleaching). Moreover, exposure of microinjected cells to excessive excitation light before photobleaching resulted in a diffuse distribution of rh-tubulin. In this case also, no mobile fluorescent components could be detected after photobleaching.

Analysis of the Fringe Pattern Fluorescence Photobleaching Data

The decay in contrast recorded for 300 s by scanning forth and back the analyzing fringe pattern (Davoust et al., 1982) was fitted by two terms: a rapid exponential decay and a linear slope which was considered as the initial asymptote of a very slow exponential decay. The first component was characterized by a short exponential decay time constant (t) and led to the determination of the diffusion coefficient D of free tubulin: $D = d^2/(4\pi^2 \cdot \tau)$ where d is the interfringe distance expressed in cm and τ the exponential decay expressed in seconds. The slow component was characterized by a time-dependent linear loss of contrast expressed in percent of contrast lost per second. By extrapolation to the loss of a normalized contrast of 100%, one finds a time-scale equal to the exponential decay time constant measured from the initial asymptote of a very slow exponential decay. The half-life is simply related to this normalized time-constant (t_{slope}): $t_{1/2} = t_{slope} \cdot \mathrm{Log_e}(2)$. This one parameter fit of the slow decay was chosen for the sake of simplicity and turned out to be very sensitive to calibration experiments where extreme conditions were used, such as the nocodazole-induced depolymerization of microtubules or stabilization of microtubules with taxol. It provided us with a semiquantitative measurement of microtubule turnover, averaged over a whole cell. More sophisticated multiparametric analyses of the slow decay would in principle be more accurate, but they turned out to have clear drawbacks such as the high correlation of the various parameters fitted from noisy curves. In fact, more sophisticated multiexponential fitting procedures were avoided because of the strong correlation found between the setting of the parameters. This was due to the fact that the standard recording time of 300 s was usually shorter than the half-life of the microtubules and therefore only the initial slope of this slow decay was measured during the 300 s after pattern photobleaching. Periods of recording were limited to 300 s to avoid photobleaching artefacts and problems with microscope stage instability.

Immunofluorescence Labeling of Cells

Microtubules were labeled in cells with murine monoclonal antibodies either against α-tubulin (Amersham Buchler, Braunschweig, FRG) or against the tyrosinated carboxyterminus of α-tubulin (1A2; Kreis, 1987) and fluorescein labeled antibodies against mouse immunoglobulins, as described (Bré et al., 1987; Kreis, 1987). To obtain maximal contrast of rhodamine-labeled microtubules, microinjected cells were usually preextracted with detergent before fixation in methanol at −20°C (Bré et al., 1987). Fluorescence microscopy and photography was performed as described (Kreis, 1987).

Microphotometric Measurements of Fluorescence in Microinjected Cells

Intensities of rhodamine- and fluorescein-labeled microtubules were measured in preextracted, double-labeled cells using a photon counting system (EMI T1500; Thorn) adapted to the fluorescence microscope. Linearity of the system was verified by varying the intensity of the excitation light beam with neutral density filters. Fluorescence was measured in single cells by

1. *Abbreviations used in this paper*: MAP, microtubule-associated protein; rh-tubulin, rhodamine-labeled tubulin.

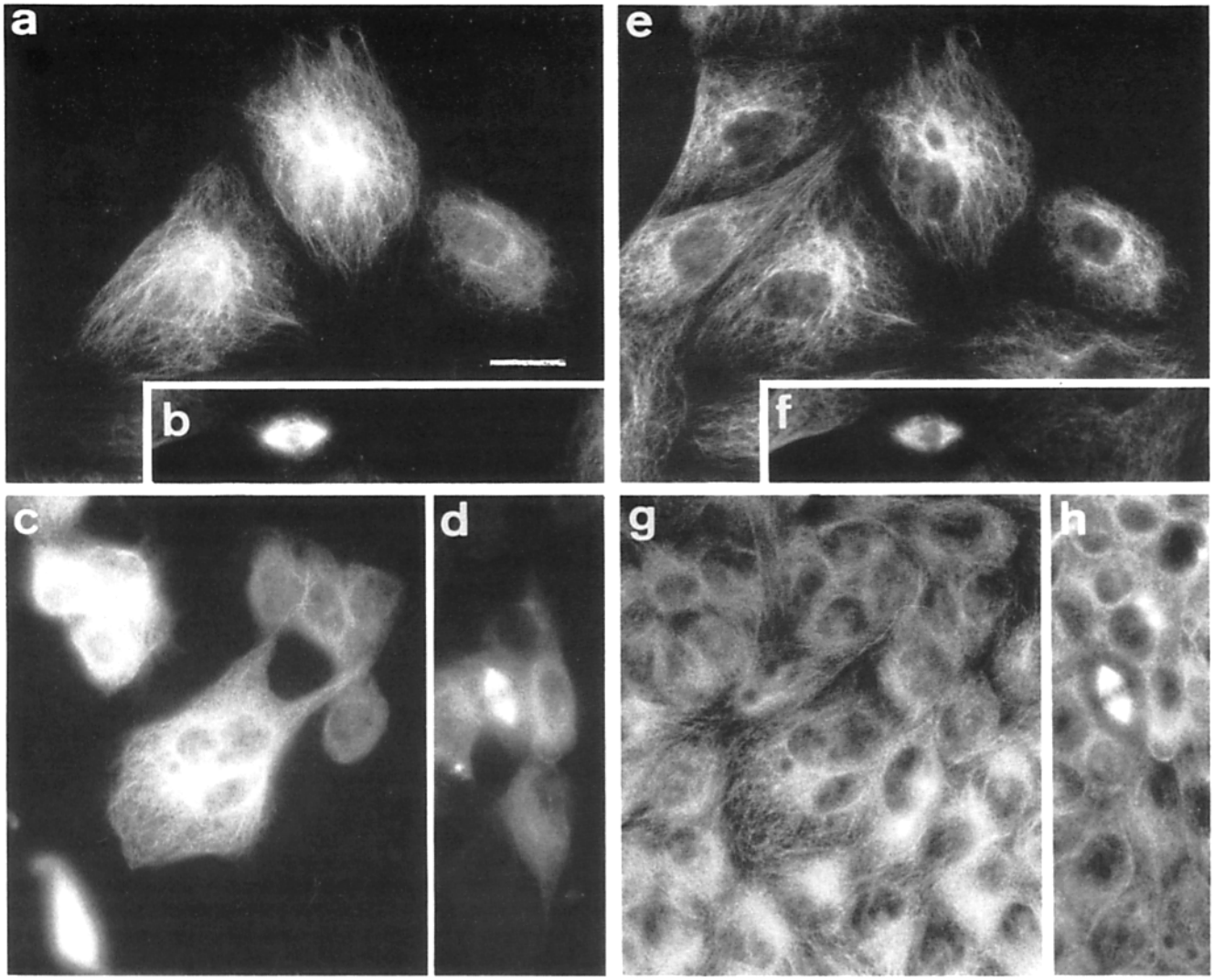

Figure 1. Microinjected fluorescently labeled tubulin incorporates into all cellular microtubules. Sparse (*a*, *b*, *e*, and *f*) and confluent (*c*, *d*, *g*, and *h*) MDCK cells were microinjected with rh-tubulin (*a–d*), preextracted and fixed after 2 h (*a*, *c*, *e*, and *g*) or 24 h (*b*, *d*, *f*, and *h*), and labeled with fluorescein using a monoclonal antibody against tyrosinated α-tubulin (*e–h*). Rh-tubulin could be detected in all interphase microtubules (*a* and *c*) visualized by immunofluorescence labeling (*e* and *g*), and it clearly labeled the spindle microtubules up to at least 24 h after injection (*b* and *d*). Microtubules in densely confluent MDCK cells were only poorly resolved. Bar, 20 μm.

reducing excitation and detection light beams with the field iris of the microscope and a pinhole (3-mm-diam) placed in the intermediate image plane of the microscope before the photomultiplier. This confocal arrangement using large pinholes ensured that only the fluorescence of the cell of interest is measured (Warren et al., 1987). Unspecific background fluorescence was determined in cells labeled with secondary antibodies only.

Results

Rhodamine-labeled Tubulin Incorporates into All Cellular Microtubules

rh-tubulin was microinjected into Vero and MDCK cells at different stages of confluency and cells were fixed afterwards at various time points to analyze the incorporation of the fluorescently tagged protein into microtubules. Virtually all interphase microtubules were labeled with rh-tubulin 1 h postinjection and fluorescent microtubules could be detected in sparse or confluent cells for >24 h (Fig. 1, *a*, *c*, *e*, and *g*; for microinjected Vero fibroblasts see also Kreis, 1987). Injected rh-tubulin incorporated also into the mitotic spindle microtubules up to at least 1 d after injection (Fig. 1, *b*, *d*, *f*, and *h*). These experiments demonstrate that rh-tubulin can be used as a reporter protein for analyzing the dynamic properties of endogenous tubulin in vivo and that dynamic cellular processes, such as mitosis, appear not to be disturbed by the microinjection process.

Dynamic Properties of Tubulin in Sparse Vero and MDCK Cells

The dynamic properties of microtubules were measured by fringe pattern fluorescence photobleaching as described previously (Davoust et al., 1982; Cosson, Pepperkok, Back, and Davoust, manuscript submitted for publication) in living interphase and mitotic Vero and MDCK cells microinjected

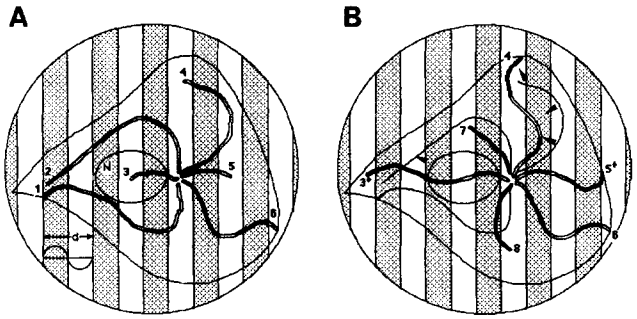

Figure 2. Disappearance of fringe pattern fluorescence contrast is due to diffusion of soluble free rh-tubulin, movement of microtubules, and microtubule depolymerization. Fluorescently labeled microtubules, immediately after fringe pattern fluorescence photobleaching and after subsequent fluorescence recovery, are shown schematically in *A* and *B*, respectively; remaining fluorescent microtubule segments are depicted as filled, and bleached segments as open segments. Fringe pattern fluorescence contrast (measured by the attenuated fringe pattern) decreases only when bleached microtubules depolymerize (microtubule *1* and *2*) or when a microtubule moves away from its initial position (microtubule *4* in *B*); newly polymerized microtubule segments are evenly labeled with rh-tubulin and thus, do not contribute to changes in overall fluorescence contrast (microtubules 3^+, 5^+, *7*, and *8* in *B*). *N*, nucleus *d* indicates the interfringe distance.

with rh-tubulin. Disappearance of the fluorescence contrast photobleached into the labeled cells can in principle occur in three ways (as schematically illustrated in Fig. 2): by diffusion of soluble components in the cytoplasm, by movement of microtubules across the fringe pattern (e.g., microtubule *4* in Fig. 2), or by depolymerization of microtubules (e.g., microtubules *1* and *2* in Fig. 2). After fluorescence photobleaching, assembly of microtubules that are evenly labeled does not change the remaining fluorescence contrast (e.g., microtubules 3^+, 5^+, *7*, and *8* in Fig. 2). Since the diffusion of free tubulin in the cytoplasm is much faster than assembly of microtubules, recruitment of rh-tubulin for polymerization into microtubules does not influence the slow decay of the fluorescence pattern contrast.

The accuracy and validity of the fluorescence photobleaching method used in this study, and controls for avoiding potential artifacts (see Vigers et al., 1988, for example) were assessed in several independent ways. (*a*) We have labeled tubulin with the primary amino group-reactive sulfonyl-chloride derivative of rhodamine lissamine B (fluorochrome to protein ratio of 0.2), which has proven to be a good probe for similar experiments with actin (Kreis et al., 1982). Furthermore, in contrast to Vigers et al. (1988), who labeled phosphocellulose purified tubulin, we labeled tubulin in the microtubule polymer containing the MAPs, which we expected to protect functionally important domains of tubulin. rh-tubulin was purified and separated from the MAPs after rhodamine labeling (Kreis, 1987). (*b*) The fringe pattern used for fluorescence photobleaching and recording was chosen to cover whole cells, thus an average of overall microtubule dynamics within a given cell could be determined. (*c*) The intensity of the laser pulse for bleaching was chosen so that only ~10% of the cytoplasmic fluorescence was photobleached. Due to the increase in sensitivity associated with the spatial averaging of the contrast of the pattern these low bleaching values are sufficient. 10% contrast cannot be detected by classical imaging and recording, still it is sufficient to create an averaged contrast that can be recorded as a function of time by scanning forth and back the analyzing fringe pattern during the detection phase (Davoust et al., 1982). Repeated fluorescence photobleaching experiments on same cells gave the same results. (*d*) Recording and quantitation of the redistribution of fluorescence signals after bleaching was done with minimal laser light (~10^4-fold attenuated laser); under these illumination conditions virtually no bleaching of fluorescence (<1% within 5 min of continuous recording) was detected. (*e*) The integrity of the microtubule pattern was controlled in the living cells at the end of each photobleaching experiment. Rearrangement, growth or depolymerization of microtubules could be observed after fluorescence photobleaching. Moreover, microtubules remained sensitive to depolymerization by nocodazole and subsequent repolymerization (data not shown). (*f*) Fringe pattern fluorescence photobleaching of rh-tubulin in cells treated with the microtubule stabilizing agent taxol clearly showed that the stability of microtubules was not impaired by mechanical breakage.

Fringe pattern fluorescence photobleaching was performed at various time points after microinjection of cells with rh-tubulin, and data were subsequently obtained and analyzed as described previously for microinjected rhodamine-labeled clathrin (Cosson, Pepperkok, Back, and Davoust, manuscript submitted for publication). An interfringe distance of 10 μm (*d*; see Fig. 2 *A*) was used in most experiments. Note that due to the sine profile of the illumination

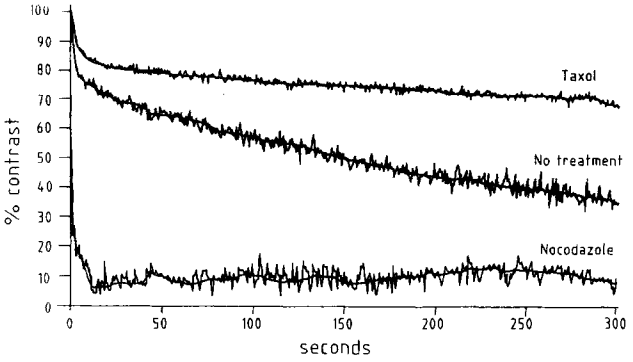

Figure 3. Dynamic properties of rh-tubulin in MDCK cells. 2-d-old sparse MDCK cells were microinjected with rh-tubulin and analyzed 2 h after injection by fringe pattern fluorescence photobleaching. Individual cells were photobleached and analyzed. The dynamic properties of rh-tubulin were measured in control cells (no treatment) or in cells pretreated with microtubule organization-disrupting drugs (nocodazole and taxol). Disappearance of fringe pattern fluorescence contrast was measured as a function of time as described in Materials and Methods, and the averaged kinetics of recovery of at least 20 measurements in different cells were calculated. Two components of rh-tubulin could be distinguished with respect to their rates of recovery, a fast component (free rh-tubulin) and a slow component (rh-tubulin associated with microtubules) with almost linear kinetics with $t_{1/2}$ in the order of seconds and minutes, respectively. Cells were treated with nocodazole starting 4 h, or with taxol starting 1 h before fluorescence photobleaching was performed. In nocodazole treated cells >90% rh-tubulin was shifted into the pool with fast recovery kinetics, whereas taxol treatment of cells strongly inhibited decay of fringe pattern fluorescence contrast.

Table I. Diffusion of Microinjected Rhodamine-labeled Proteins in Vero and MDCK Cells

Injected proteins	Cells	D^*	% Contrast‡
		10^{-8} cm²/s	
Rh-tubulin	Vero	1.61 ± 0.10	38 ± 5 (31)
	Vero (nocodazole)	2.35 ± 0.21	90 ± 4 (14)
	MDCK	1.34 ± 0.12	35 ± 3 (12)
	MDCK (nocodazole)	2.13 ± 0.18	80 ± 4 (12)
Rh-BSA	MDCK	1.39 ± 0.10	81 ± 4 (18)

Fringe pattern fluorescence photobleaching was performed and analyzed in sparse cells 1 h after microinjection as described in Materials and Methods. Nocodazole treatment of cells was as described in Materials and Methods. Data are expressed as the mean ± SD.

* The diffusion coefficient D was calculated as described (Davoust et al., 1982).

‡ The percentage of free rh-tubulin was determined from the intercept of the slope of the slow component with the ordinate (see Fig. 3). Numbers of cells analyzed are given in brackets.

beam light intensities vary steeply from 0 to 100% over a distance of $d/2$. This means that molecular motions of the order of d/π can be detected by pattern photobleaching.

A typical example of a photobleaching experiment is shown in Fig. 3. No significant differences in the rate of fluorescence recovery after photobleaching could be detected when cells were analyzed 1–24 h after injection of rh-tubulin (data not shown). Since virtually all microtubules were labeled within 2 h after injection, and thus rh-tubulin had equilibrated with the endogenous pool of protein, fluorescence photobleaching experiments were performed at this time point, unless indicated otherwise. Two components with different mobilities could be distinguished, one with high mobility ("fast component"; diffusion coefficient D = 1.3–2.4 × 10^{-8} cm²/s; Table I) and one with low mobility ("slow component"; $t_{1/2}$ of several minutes). The component with fast mobility is free rh-tubulin, since its pool (30–40% in control cells) could be maximally increased, to up to 95%, by treatment of cells with the microtubule depolymerizing drug nocodazole (Fig. 3). In addition, the amount of the fast component was reduced by treatment of cells with the microtubule stabilizing agent taxol to <20% (Fig. 3). These results taken together demonstrate that the slow component must be rh-tubulin associated with microtubules. Since the method of fringe pattern fluorescence photobleaching used here determines rates of disappearance of contrast (Davoust et al., 1982), these rates correspond to the kinetics of dissociation of rh-tubulin from microtubules, which correlates with the rates of microtubule disassembly (we assume that exchange of tubulin occurs at microtubule ends only). 15–30 s after bleaching a linear slope of slow fluorescence contrast decay was reached (slow component), suggesting microtubule depolymerization with an average half-time of several minutes (Fig. 3; for a more detailed analysis see below). Once disassembled from photobleached microtubules, the rh-tubulin can diffuse rapidly in the cytoplasm and participate in the repolymerization of microtubules. Since diffusion of bleached and unbleached rh-tubulin is very fast compared with the average rate of microtubule depolymerization, it does not influence the analysis of the slow decay of fluorescence contrast.

Turnover of mitotic spindle microtubules was significantly accelerated in comparison to interphase microtubules (Table II). Results obtained from four different mitotic cells suggest that microtubules have a $t_{1/2}$ of 15 ± 3 s (Table II). Obviously the sample size was small, but finding mitotic cells and performing fluorescence photobleaching experiments on them was technically difficult. The values for spindle microtubule half-lives determined by this method, however, were in good agreement with the values of 15–40 s measured in other systems and with different methods (Mitchison et al., 1986; Salmon et al., 1984*a*,*b*; Wadsworth and Salmon, 1986).

We observed no significant differences in the diffusion coefficient and the amounts of soluble tubulin in sparse or confluent Vero and MDCK cells, and these values were similar to rhodamine-labeled BSA microinjected into cells as a marker for soluble cytoplasmic protein (Table I). Mobility of soluble tubulin was increased in cells treated with nocodazole. This result may suggest that depolymerization of microtubules and disorganization or rearrangement of cytoplasmic membranous organelles decreases restrictions of diffusion of soluble components. Values of D measured here by fringe pattern fluorescence photobleaching are in good agreement with diffusion coefficients determined by other methods with other proteins in other cell systems (Barisas and Leuther, 1979; Kreis et al., 1982; Luby-Phelps et al., 1988; Salmon et al., 1984*c*; Scherson et al., 1984; Wang et al., 1982; Wojcieszyn et al., 1981).

Microtubules Are Stabilized in Confluent MDCK But Not Vero Cells

The dynamic properties of fluorescently labeled microtubules were further investigated in sparse and confluent interphase Vero and MDCK cells. For this purpose we determined the half-times of contrast decay of the slow rh-tubulin component after fluorescence photobleaching in these cells

Table II. Correlation of Microtubule Dynamics and Cell Density

Cells	Free rh-tubulin*	Microtubule half-life‡
Vero cells	%	*min*
Sparse	33 ± 2.0	10.9 ± 1.1 (22/1)
Confluent	35 ± 3.3	10.4 ± 1.1 (21/2)
Sparse (taxol)	21 ± 2.8	24.1 ± 1.7 (11/7)
MDCK cells		
Sparse	39 ± 2.4	8.9 ± 0.6 (36/1)
Confluent	38 ± 3.4	16.3 ± 0.9 (25/9)
High confluency	32 ± 2.8	16.7 ± 1.2 (35/14)
Sparse (taxol)	19 ± 2.7	21.9 ± 2.1 (11/7)
Mitotic§	N.D.	0.25 ± 0.05 (4)

Fringe pattern fluorescence photobleaching was performed and analyzed 2 h post-injection of cells with rh-tubulin as described in Materials and Methods. Drug treatment of cells was as described in Materials and Methods. Examples of sparse and confluent cells used for fluorescence photobleaching experiments are shown in Fig. 1. Data are expressed as the mean ± SD.

* The amount of free rh-tubulin was determined as described in Table I.

‡ Microtubule half-lives were determined from the linear slope of the slow component (see Fig. 3). Numbers of cells analyzed are given in brackets (first number); the second number gives the cells with $t_{1/2}$ of >25 min. The populations of cells with different microtubule half-lives were further analyzed in Fig. 4.

§ All cells analyzed were in anaphase.

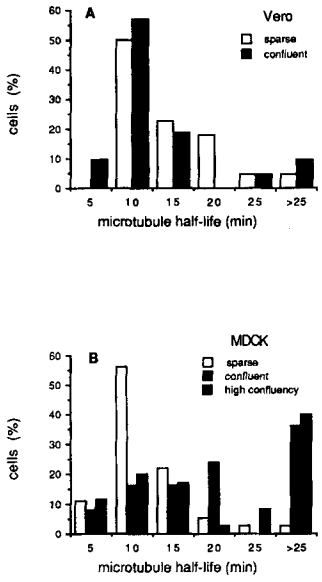

Figure 4. Analysis of the dynamic properties of microtubules in populations of sparse and confluent Vero (*A*) and MDCK (*B*) cells. Fringe pattern fluorescence photobleaching was performed on single cells and analyzed as described in the legend to Fig. 2 (see also Table II). Typical examples of microinjected sparse or confluent MDCK cells are shown in Fig. 1 (see also Kreis, 1987 for rh-tubulin-injected Vero cells). The average microtubule half-lives were calculated on individual cells from the kinetics of the component with slow recovery, and cells were grouped according to their microtubule half-lives. The distribution of cells with respect to the $t_{1/2}$ of microtubules was similar in sparse Vero and MDCK, and in confluent Vero cells, with an average $t_{1/2}$ of 9–11 min (see Table II). A distinct shift in the distribution of cells towards longer $t_{1/2}$ of microtubules was observed in confluent or highly confluent MDCK cells with domes; similar average $t_{1/2}$ of ~16 min were measured in cells at both densities.

(see Fig. 3). The average microtubule half-lives in sparse Vero and MDCK, and in confluent Vero cells was ~10 min (Table II). In MDCK cells, a clear drop in microtubule turnover rates was observed as they reached confluency. MDCK cells grown to confluency or to high confluency (monolayer cells exhibiting "domes") had on a cell average microtubule half-lives of 16–17 min (Table II). Maximal stabilization of microtubules to average $t_{1/2}$s of 24 and 22 min could be obtained by treatment of sparse Vero and MDCK cells, respectively, with taxol (Table II). These average values clearly underestimate the real $t_{1/2}$s of the microtubules, since values >25 min could not be distinguished by this method due to thermal motions of the cells and overall long-term instability of the microscope stage and of the interferometric system that forms the fringe pattern. In fact, the two-thirds of microtubules with $t_{1/2}$s >25 min were arbitrarily set to 25 min for averaging (Table II).

The population of microinjected cells was further analyzed with respect to the distribution of cells with different average microtubule stabilities. About 60% of the sparse Vero and MDCK cells had an average $t_{1/2}$ of microtubules of ~10 min (Fig. 4; see also Table II). No significant difference in the distribution of cells with different microtubule half-lives was detected when sparse and confluent Vero cells were compared (Fig. 4 *A*). In contrast to the Vero cells, reaching cell confluency had a strong effect on microtubule stability in MDCK cells. Indeed, the proportion of MDCK cells with a very slow microtubule turnover ($t_{1/2} \geq 20$ min) increased from 10% in sparse cells to over 60% in confluent or highly confluent cells (Fig. 4 *A*). Apparently, therefore, microtubule stabilization occurred after establishment of cell–cell contacts and formation of junctions in the MDCK cells.

The Rate of Microtubule Assembly Is Reduced in Confluent MDCK Cells

As an additional, independent approach to determine changes in the dynamic properties of microtubules in sparse and confluent MDCK cells, we have measured the rate of incorporation of rh-tubulin into interphase microtubules (see Bré et al., 1990). Sparse and confluent MDCK cells were microinjected with rh-tubulin and the ratio of microtubule-associated rh-tubulin and total endogenous tubulin in microtubules, labeled by immunofluorescence, was determined on a cell average at different time points after injection and preextraction of soluble protein from the cells. The ratio of polymerized injected rh-tubulin over fluorescein-labeled total endogenous microtubules reached the same plateau at 15–20 and 60 min in sparse and confluent MDCK cells, respectively; 50% of endogenous microtubules were labeled with rh-tubulin after ~10 and ~17 min in sparse and confluent MDCK cells, respectively (Fig. 5 *A*). Thus, the average rate of tubulin incorporation is about twofold reduced in confluent MDCK cells (Fig. 5 *A*). This result is in good agreement with the data obtained by fluorescence photobleaching, where rates of disassembly of microtubules were determined. Interestingly, a similar reduction in the rate of assembly was determined when microtubule-associated injected rh-tubulin was compared with endogenous tyrosinated microtubules in sparse and confluent cells ($t_{50\%}$ ~5 and 8 min, respectively; Fig. 5 *B*). This observation may indicate that tyrosinated microtubules are stabilized as MDCK cells grow to confluency and establish cell–cell contacts. This result would confirm our previous data using nocodazole-induced microtubule depolymerization to measure stabilization of microtubules in confluent MDCK cells (Bré et al.,

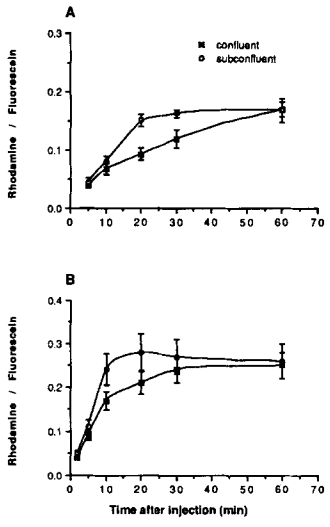

Figure 5. The rate of association of rh-tubulin with the microtubule network is reduced in confluent MDCK cells as compared to sparse cells. Sparse and confluent MDCK cells were microinjected with rh-tubulin, preextracted at different time points of culture after injection, fixed and immunolabeled with fluorescein with mAbs against α-tubulin (*A*) or the carboxy-terminal tyrosin of α-tubulin (*B*). The signals (arbitrary units) of cell associated microinjected rh-tubulin and fluorescein-labeled total endogenous tubulin were measured photometrically as described in Materials and Methods. 20–35 individual cells were analyzed for each time point, except for the early time points (2 and 5 min) where 7–18 cells were analyzed. The ratio of rh-tubulin labeling over fluorescein-labeled endogenous microtubules reached a plateau at 20–30 min and 60 min in sparse and confluent MDCK cells, respectively (*A*). Incorporation into tyrosinated microtubules was faster and plateaus were reached after 15–20 and 30–60 min, respectively (*B*).

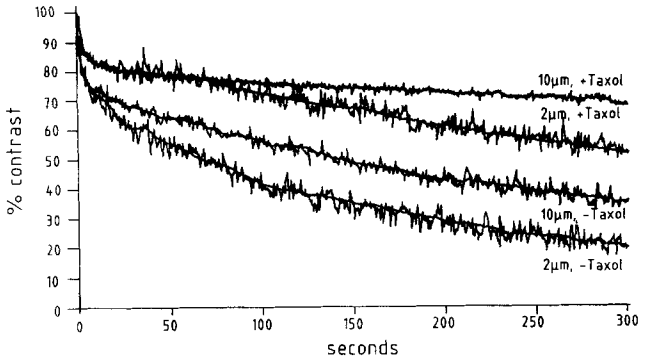

Figure 6. The interfringe distance dependent rate of disappearance of fringe pattern fluorescence contrast depends on mobility and not on depolymerization of microtubules. Fluorescence photobleaching experiments were done analogous as described in the legend to Fig. 3 on sparse MDCK cells with or without taxol treatment with interfringe distances of 2 and 10 μm. A significant rate of fluorescence recovery is observed at an interfringe distance of 2 μm, in contrast to 10 μm, in the presence of 10 μM taxol. This difference in rate of recovery is similar to the difference in recovery when 2 and 10 μm interfringe distances are compared without taxol treatment of the cells.

1987; see also Webster et al., 1990). Furthermore, these results suggest that the average turnover of tyrosinated microtubules is about twice faster than the total endogenous microtubules.

Restriction of Microtubule Mobility in Confluent MDCK Cells

Further information on the dynamic properties of microtubules could be obtained by fluorescence photobleaching of cells labeled with rh-tubulin by varying the interfringe distance (see Fig. 2) of the fringe pattern between 1.4 and 20 μm. As mentioned earlier, this means that we are probing motion over distances of 0.4–6 μm in the cells. The kinetics of apparent relaxation of contrast in both sparse Vero and MDCK cells clearly depended on the interfringe distance used in the bleaching experiments. Disappearance of contrast was fastest when smallest interfringe distances were used and a plateau was observed at ~10 μm (data not shown; see also Fig. 6). The following two conclusions were drawn from this observation. Firstly, at interfringe distances of 10 μm or larger, relaxation of contrast coincided directly with the disassembly of labeled microtubules. Secondly, at interfringe distances <10 μm, spatial mobility of microtubules in the micrometer range contributed significantly to the long term disappearance of the fringe pattern contrast photobleached into the interphase microtubules (see for example microtubule *4* in the scheme in Fig. 2). Taxol did not abolish the differences in relaxation of contrast in Vero (not shown) and MDCK cells when the interfringe distance was changed (Fig. 6). Taxol clearly stabilizes the microtubules (Fig. 3), and therefore, we assume that only minimal relaxation of contrast can occur under these conditions by tempered depolymerization of microtubules. Thus, movement of microtubules in the cytoplasm can be measured by using small interfringe distances. The critical distance below which microtubule movement can be detected is ~3 μm (10 μm/π). On larger distance scales microtubule depolymerization is faster than the "sweeping" movements of whole microtubules.

No difference in this movement of microtubules was observed when subconfluent and confluent Vero cells were compared. Movement of labeled interphase microtubules, however, was completely abolished when MDCK cells had reached confluency. In contrast to sparse cells, no significant differences in the kinetics of disappearance of contrast could be observed when confluent MDCK cells were photobleached with an interfringe distance of 2 and 10 μm (Fig. 7).

Discussion

We have applied the method of fringe pattern fluorescence photobleaching (Davoust et al., 1982) to analyze the dynamic properties of microtubules in sparse and confluent Vero fibroblasts or MDCK epithelial cells. Taken together, these experiments show that microtubules are stabilized in MDCK cells, but not in Vero cells, as they reach confluency.

The validity of these data depends both on the quality of the reporter probe (rh-tubulin) and on the reliability of the method of measurement (fringe pattern fluorescence photobleaching). The following observations strongly suggest that the fluorescently modified tubulin probe (rh-tubulin) is a faithful marker of the dynamic properties of the endogenous cellular pool of tubulin. In vitro, rh-tubulin and unmodified tubulin have virtually identical polymerization characteristics (Kreis, 1987). The complete microtubule network remained fluorescently labeled for longer than one day after microinjection of rh-tubulin, and rh-tubulin did not associate with any other cytoplasmic structures (see also Kreis, 1987). Furthermore, rh-tubulin incorporated into all cellular microtubules, including the microtubules of the mitotic spindle, during at least one day after microinjection. Thus, the recipient cells do not discriminate between microinjected rh-tubulin and endogenous tubulin, showing that the fluorescent tracer can be used as a reporter probe for monitoring the true dynamic properties of cellular tubulin.

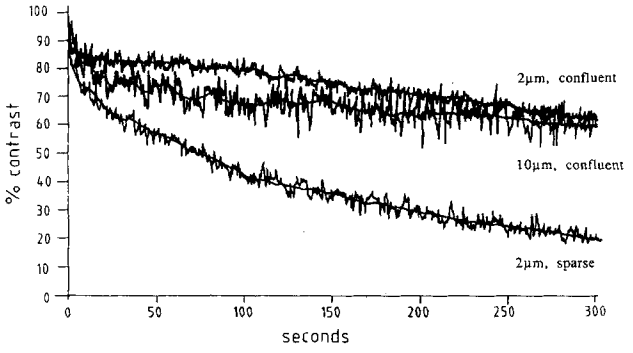

Figure 7. Mobility of microtubules is restricted in confluent MDCK cells. Fringe pattern fluorescence photobleaching on sparse and confluent MDCK cells was performed 2 h after microinjection of cells with rh-tubulin as described in the legend to Fig. 3 with 2 and 10-μm interfringe distances. In contrast to sparse cells (see Fig. 6) no significant difference in the rate of disappearance of fringe pattern fluorescence contrast could be observed in confluent MDCK cells.

Previous studies have indicated that the experimental parameters for fluorescence photobleaching need to be carefully controlled to prevent photodamaging of labeled microtubules (Vigers et al., 1988). More recently, Olmsted et al. (1989) have used the same method of fluorescence photobleaching discussed by Vigers et al. (1988) to measure the dynamic properties of MAPs in vivo and, in contrast to the previous experiments with labeled tubulin, they found no significant perturbation of microtubule integrity. An appropriate choice of fluorochrome for labeling of the tracer protein, a low molar ratio of fluorochrome to protein and a mild labeling procedure performed on intact microtubules is obviously of critical importance in these experiments. The following reasons convinced us that we measured the true dynamic properties of microtubules in vivo by the approach used in this study. We obtained identical microtubule half-lives by subsequent fluorescence photobleaching experiments on the same cells. Microtubules appeared to remain undisturbed after photobleaching and during the subsequent measurement of fluorescence recovery. Furthermore, rates of incorporation of rh-tubulin into microtubules and rates of microtubule depolymerization, were very similar, although measured by completely different methods. In addition, the average rates of microtubule dynamics determined in this study are comparable to published data measured by other methods (Cassimeris et al., 1988; Kreis, 1987; Sammak et al., 1987; Saxton et al., 1984; Schulze and Kirschner, 1986; Wadsworth and McGrail, 1990).

Three components of rh-tubulin with different dynamic properties can be distinguished and they may be attributed to diffusion of soluble tubulin, mobility of microtubules in the cytoplasm, and depolymerization of microtubules. The pool of soluble tubulin in Vero and MDCK cells remained constant at a level of 30–40% of the total endogenous pool and did not vary significantly at the various stages of cell confluency. Treatment of cells with taxol reduced the fraction of soluble cytoplasmic tubulin to ~20%, whereas nocodazole increased the mobile fraction of rh-tubulin to up to 90%. Interestingly, by varying the interfringe distance, mobility of microtubules could be measured in the cytoplasm of Vero and sparse MDCK cells. This movement of microtubules must be in the range of <3 μm, since it was not detected at interfringe distances of 10 μm or larger. It reached the slope of the slow component within ~1 min (Fig. 6), suggesting that a significant fraction of cytoplasmic microtubules may move on average at several micrometers per minute. Mobility of microtubules has previously been shown in living cells fluorescently labeled with microinjected derivatized tubulin (Sammak and Borisy, 1988). Mobility of microtubules leading eventually to bending may also be inferred for example from the very sinuous morphology of "old" detyrosinated microtubules (see for example Gundersen et al., 1984; Kreis, 1987). Active movement of microtubules may occur along a stable cytoplasmic scaffold (other cytoskeletal structures or intracellular membranes). This micromobility of microtubules is halted in confluent MDCK cells. A plausible explanation for this observation is stable anchoring of the microtubules within the cytoplasmic matrix or association with cellular membranes. We cannot exclude the possibility, however, that mobility of microtubules in densely grown, more columnar MDCK cells occurs predominantly vertically. No vertical resolution is possible in the fluorescence recovery measurements after photobleaching. The fringe pattern sections the cells with vertical planes of light and we can thus only measure motions that occur in the horizontal plane. Such a restriction of microtubule mobility was not detected in dense Vero cells. Since also densely confluent Vero cells are more columnar than sparse ones, we consider this latter possibility as more unlikely.

The turnover of microtubules is reduced about twofold as the epithelial MDCK cells reached cell confluency and established extensive cell–cell contacts (Simons and Fuller, 1985; Rodriguez-Boulan and Nelson, 1989). This conclusion was obtained independently by measuring disappearance of labeled microtubules using fringe pattern fluorescence photobleaching methods and by determining the average rates of microtubule assembly by quantitating association of microinjected rh-tubulin with interphase microtubules. Interestingly, the instantaneous elongation rates of individual microtubules were not significantly altered when MDCK cells established cell–cell contacts and reached confluency (Bré et al., 1990). Therefore, the increased microtubule half-life and the slower average rate of incorporation of rh-tubulin into microtubules in confluent MDCK cells strongly suggest that the frequency with which microtubules alternate between growing or shrinking phases is reduced, rather than the rates of growth at microtubule ends. In addition, factors unknown so far may modulate microtubule dynamics. The stabilization of microtubules in confluent MDCK cells probably plays a role in the reorganization of the microtubule network that occurs during differentiation of epithelial cells into a polarized monolayer. Indeed, this accompanies the dispersion of the microtubule organizing center and separation of centrioles (Bacallao et al., 1989; Buendia et al., 1990), as well as microtubule reorientation into longitudinal bundles arranged along the apicobasal axis of the columnar polarized cells (Bacallao et al., 1989). Such reorganizations of cytoplasmic structures have not been observed in confluent Vero cells. So far, fluorescence photobleaching experiments cannot be performed on highly polarized MDCK cells grown on filters (Simons and Fuller, 1985) because of intense stray light. It should be interesting to find out whether microtubules in filter-grown MDCK cells reach maximal stabilities, comparable to those obtained by taxol treatment of cells. Further developments may allow us to use confocal microscopes for such fluorescence photobleaching experiments in the near future.

Clearly, cell–cell contact formation induces stabilization of microtubules in MDCK cells (see also Bré et al., 1987). Wadsworth and McGrail (1990) recently reported that microtubule disassembly occurs faster in fibroblasts ($t_{1/2}$ of 4 min) than in epithelial cells ($t_{1/2}$ 18 and 72 min), using nocodazole to block microtubule assembly. Unfortunately, microtubule disassembly rates were not analyzed with respect to cell confluency in this analysis (Wadsworth and McGrail, 1990). Several factors may contribute to stabilization of microtubules in confluent MDCK cells. Interaction of microtubules with other cytoskeletal elements or anchoring of microtubules at membranes may reduce the rates of microtubule turnover. Tubulin in such transiently stabilized microtubules would remain exposed for longer periods of times to cytoplasmic enzyme activities, and therefore, become more prone to post-translational modifications (see for example Bré et al., 1987; Kreis et al., 1987; Schulze et al.,

1987; Webster and Borisy, 1989; see also Bré et al., 1990). Additionally, modified tubulin may exhibit altered properties for binding of cellular, microtubule stabilizing components. Alternatively, it may be postulated that cell–cell contact formation in confluent cells induces the synthesis or activation of a specific class of microtubule stabilizing proteins in MDCK cells. Induction of specific classes of MAPs that are involved in stabilizing or bundling of microtubules could clearly be demonstrated in differentiating neuronal cells (Drubin et al., 1985; for a recent review see for example Matus, 1988). Analysis of posttranslational modifications of microtubule components and the possibility of induction of microtubule stabilizing proteins upon cell–cell contact formation will help to further characterize the molecular mechanisms underlying the specific stabilization of microtubules in MDCK cells in more detail.

We would like to thank Eric Karsenti for stimulating discussions and Wilhelm Ansorge for providing the microinjection facility. We appreciated Jan De Mey, Stephen Fuller, Eric Karsenti, and Kai Simons' (all at EMBL) helpful comments on the manuscript and Petra Riedinger's help with preparing graphs for figures. Taxol was obtained from Dr. N. Lomax (Department of Health and Human Services, National Institutes of Health).

Received for publication 28 May 1990 and in revised form 15 August 1990.

References

Ansorge, W., and R. Pepperkok. 1988. Performance of an automated system for capillary microinjection into living cells. *J. Biochem. Biophys. Methods.* 16:283–292.

Baas, P. W., L. A. White, and S. R. Heidmann. 1987. Microtubule polarity reversibly accompanies regrowth of amputated neurites. *Proc. Natl. Acad. Sci. USA.* 84:5272–5276.

Bacallao, R., C. Antony, C. Dotti, E. Karsenti, E. H. K. Stelzer, and K. Simons. 1989. The subcellular organization of Madin-Darby canine kidney cells during the formation of a polarized epithelium. *J. Cell Biol.* 109:2817–2832.

Barisas, B. G., and M. D. Leuther. 1979. Fluorescence photobleaching recovery measurement of protein absolute diffusion coefficients. *Biophys. Chem.* 10:221–229.

Black, M. M., and P. Keyser. 1987. Acetylation of alpha-tubulin in cultured neurons and the induction of alpha-tubulin acetylation in PC12 cells by treatment with nerve growth factor. *J. Neurosci.* 7:1833–1842.

Black, M. M., and P. W. Baas. 1989. The basis of polarity in neurons. *Trends Neurosci.* 12:211–214.

Bré, M.-H., T. E. Kreis, and E. Karsenti. 1987. Control of microtubule nucleation and stability in Madin-Darby canine kidney cells: the occurance of noncentrosomal, stable detyrosinated microtubules. *J. Cell Biol.* 105:1283–1296.

Bré, M.-H., R. Pepperkok, A. M. Hill, N. Lavilliers, W. Ansorge, E. H. K. Stelzer, and E. Karsenti. 1990. Regulation of microtubule dynamics and nucleation during polarization in MDCK II cells. *J. Cell Biol.* 111:3013–3021.

Buendia, B., M.-H. Bré, G. Griffiths, and E. Karsenti. 1990. Cytoskeletal control of centrioles movement during the establishment of polarity in Madin-Darby canine kidney cells (MDCK). *J. Cell Biol.* 110:1123–1135.

Cassimeris, L., N. K. Pryer, and E. D. Salmon. 1988. Real-time observations of microtubule dynamic instability in living cells. *J. Cell Biol.* 107:2223–2231.

Davoust, J., P. F. Devaux, and L. Leger. 1982. Fringe pattern photobleaching, a new method for the measurement of transport coefficients of biological macromolecules. *EMBO (Eur. Mol. Biol. Organ.) J.* 1:1233–1238.

Dinsmore, J. H., and R. D. Sloboda. 1988. Calcium and calmodulin-dependent phosphorylation of a 62 kd protein induces microtubule depolymerization in sea urchin mitotic apparatus. *Cell.* 53:769–780.

Drubin, G. D., S. C. Feinstein, E. M. Shooter, and M. W. Kirschner. 1985. Nerve growth factor-induced neurite outgrowth in PC12 cells involves the coordinate induction of microtubule assembly and assembly-promoting factors. *J. Cell Biol.* 101:1799–1807.

Drubin, D. G., and M. Kirschner. 1986. Tau protein function in living cells. *J. Cell Biol.* 103:2739–2746.

Gorbsky, G., and G. G. Borisy. 1985. Microtubule distribution in cultured cells and intact tissues: improved immunolabeling resolution through the use of reversible embedment cytochemistry. *Proc. Natl. Acad. Sci. USA.* 82:6889–6893.

Gundersen, G. G., M. H. Kalnoski, and J. C. Bulinski. 1984. Distinct populations of microtubules: tyrosinated and nontyrosinated alpha tubulin are distributed differently in vivo. *Cell.* 38:779–789.

Gundersen, G. G., S. Khawaja, and J. C. Bulinski. 1989. Generation of a stable, posttranslationally modified microtubule array is an early event in myogenic differentiation. *J. Cell Biol.* 109:2275–2288.

Houliston, E., S. J. Pickering, and B. Maro. 1987. Redistribution of microtubules and pericentriolar material during the development of polarity in mouse blastomeres. *J. Cell Biol.* 104:1299–1308.

Kanai, Y., R. Takemura, T. Oshima, H. Mori, Y. Ihara, Y. Masashi, T. Masaki, and N. Hirokawa. 1989. Expression of multiple tau isoforms and microtubule bundle formation in fibroblasts transfected with a single tau cDNA. *J. Cell Biol.* 109:1173–1184.

Karsenti, E., and B. Maro. 1986. Centrosomes and the spatial distribution of microtubules in animal cells. *Trends Biochem. Sci.* 11:460–463.

Keith, C. H., J. R. Feramisco, and M. Shelanski. 1980. Direct visualization of fluorescein-labeled microtubules in vitro and in microinjected cells. *J. Cell Biol.* 88:234–240.

Khawaja, S., G. G. Gundersen, and J. C. Bulinski. 1988. Enhanced stability of microtubules enriched in detyrosinated tubulin is not a direct function of detyrosination level. *J. Cell Biol.* 106:141–150.

Kirschner, M., and T. Mitchison. 1986. Beyond self-assembly: from microtubules to morphogenesis. *Cell.* 45:329–342.

Kreis, T. E. 1986. Microinjected antibodies against the cytoplasmic domain of vesicular stomatitis virus glycoprotein block its transport to the cell surface. *EMBO (Eur. Mol. Biol. Organ.) J.* 5:931–941.

Kreis, T. E. 1987. Microtubules containing detyrosinated tubulin are less dynamic. *EMBO (Eur. Mol. Biol. Organ.) J.* 6:2597–2606.

Kreis, T. E. 1990. Role of microtubules in the organisation of the Golgi apparatus. *Cell. Motil. Cytoskel.* 15:67–70.

Kreis, T. E., B. Geiger, and J. Schlessinger. 1982. Mobility of microinjected rhodamine actin within living chicken gizzard cells determined by fluorescence photobleaching recovery. *Cell.* 29:835–845.

Kupfer, A., D. Louvard, and S. J. Singer. 1982. Polarization of the Golgi apparatus and the microtubule-organizing center in cultured fibroblasts at the edge of an experimental wound. *Proc. Natl. Acad. Sci. USA.* 79:2603–2607.

Kupfer, A., S. J. Singer, and G. Dennert. 1986. On the mechanism of unidirectional killing in mixtures of two cytotoxic T lymphocytes: unidirectional polarization of cytoplasmic organelles and the membrane-associated cytoskeleton in the effector cell. *J. Exp. Med.* 163:489–498.

Leighton, J., L. W. Estes, S. Mansukhani, and Z. Brada. 1970. A cell line derived from normal dog kidney (MDCK) exhibiting qualities of papillary adenocarcinoma and of renal tubular epithelium. *Cancer (Phila.).* 26:1022.

Lewis, S. A., I. E. Ivanov, G.-H. Lee, and N. J. Cowan. 1989. Organization of microtubules in dendrites and axons is determined by a short hydrophilic zipper in microtubule-associated protein MAP2 and tau. *Nature (Lond.).* 342:498–505.

L'Hernault, S. W., and J. L. Rosenbaum. 1985. *Chlamydomonas* alpha-tubulin is post-translationally modified by acetylation on the epsilon-amino group of a lysine. *Biochemistry.* 24:473–478.

Lim, S.-S., P. J. Sammak, and G. G. Borisy. 1989. Progressive and spatially differentiated stability of microtubules in developing neuronal cells. *J. Cell Biol.* 109:253–263.

Luby-Phelps, K., F. Lanni, and D. L. Taylor. 1988. The submicroscopic properties of cytoplasm as a determinant of cellular function. *Annu. Rev. Biophys. Biophys. Chem.* 17:369–396.

Matus, A. 1988. Microtubule-associated proteins: their potential role in determining neuronal morphology. *Annu. Rev. Neurosci.* 11:29–44.

Mitchison, T. J. 1988. Microtubule dynamics and kinetochore function in mitosis. *Annu. Rev. Cell Biol.* 4:527–549.

Mitchison, T. J. 1989. Polewards microtubule flux in the mitotic spindle: evidence from photoactivation of fluorescence. *J. Cell Biol.* 109:637–652.

Mitchison, T., L. Evans, E. Schulze, and M. Kirschner. 1986. Sites of microtubule assembly and disassembly in the mitotic spindle. *Cell.* 45:515–527.

Morgensen, M. M., J. B. Tucker, and H. Stebbings. 1989. Microtubule polarities indicate that nucleation and capture of microtubules occurs at cell surfaces in *Drosophila*. *J. Cell Biol.* 108:1445–1452.

Okabe, S., and N. Hirokawa. 1988. Microtubule dynamics in nerve cells: analysis using microinjection of biotinylated tubulin into PC12 cells. *J. Cell Biol.* 107:651–664.

Olmsted, J. B., D. L. Stemple, W. M. Saxton, B. W. Neighbors, and J. R. McIntosh. 1989. Cell cycle-dependent changes in the dynamics of MAP2 and MAP4 in cultured cells. *J. Cell Biol.* 109:211–223.

Piperno, G., M. L. Le Dizet, and X. Chang. 1987. Microtubules containing acetylated alpha-tubulin in mammalian cells in culture. *J. Cell Biol.* 104:289–302.

Pollerberg, G. D., M. Schachner, and J. Davoust. 1986. Differentiation state-dependent surface mobilities of two forms of the neural cell adhesion molecule. *Nature (Lond.).* 324:462–465.

Rodriguez-Boulan, E., and W. J. Nelson. 1989. Morphogenesis of the polarized epithelial cell phenotype. *Science (Wash. DC).* 245:718–725.

Salmon, E. D., M. McKeel, and T. Hays. 1984*a*. Rapid rate of tubulin dissociation from microtubules in the mitotic spindle in vivo measured by blocking polymerization with colchicine. *J. Cell Biol.* 99:1066–1075.

Salmon, E. D., R. J. Leslie, W. M. Saxton, M. L. Karow, and J. R. McIntosh.

1984*b*. Spindle microtubule dynamics in sea urchin embryos: analysis using a fluorescein-labeled tubulin and measurements of fluorescence redistribution after laser photobleaching. *J. Cell Biol.* 99:2165–2174.

Salmon, E. D., W. M. Saxton, R. J. Leslie, M. L. Karow, and J. R. McIntosh. 1984*c*. Diffusion coefficient of fluorescein-labeled tubulin in the cytoplasm of embryonic cells of a sea urchin: video image analysis of fluorescence redistribution after photobleaching. *J. Cell Biol.* 99:2157–2164.

Sammak, P. J., G. J. Gorbsky, and G. G. Borisy. 1987. Microtubule dynamics in vivo: a test of mechanisms of turnover. *J. Cell Biol.* 104:395–405.

Sammak, P. J., and G. G. Borisy. 1988. Direct observation of microtubule dynamics in living cells. *Nature (Lond.).* 332:724–726.

Saxton, W. M., D. L. Stemple, R. J. Leslie, E. D. Salmon, M. Zavortink, and J. R. McIntosh. 1984. Tubulin dynamics in cultured mammalian cells. *J. Cell Biol.* 99:2175–2186.

Scherson, T., T. E. Kreis, J. Schlessinger, U. Littauer, G. G. Borisy, and B. Geiger. 1984. Dynamic interactions of fluorescently labeled microtubule-associated proteins in living cells. *J. Cell Biol.* 99:425–434.

Schulze, E., and M. Kirschner. 1986. Microtubule dynamics in interphase cells. *J. Cell Biol.* 102:1020–1031.

Schulze, E., D. J. Asai, J. C. Bulinski, and M. Kirschner. 1987. Posttranslational modification and microtubule stability. *J. Cell Biol.* 105:2167–2177.

Schliwa, M. 1984. Mechanisms of intracellular organelle transport. *In* Cell and Molecular Biology of the Cytoskeleton: Cell and Muscle Motility. Vol. 5. J. W. Shay, editor. Plenum Publishing Corp., New York. 1–82.

Simons, K., and S. D. Fuller. 1985. Cell surface polarity in epithelia. *Annu. Rev. Cell Biol.* 1:243–288.

Soltys, B. J., and G. G. Borisy. 1985. Polymerization of tubulin in vivo: direct evidence for assembly onto microtubule ends and from centrosomes. *J. Cell Biol.* 100:1682–1689.

Tassin, A.-M., M. Paintrand, E. G. Berger, and M. Bornens. 1985*a*. The Golgi apparatus remains associated with microtubule organizing centers during myogenesis. *J. Cell Biol.* 101:630–638.

Tassin, A.-M., B. Maro, and M. Bornens. 1985*b*. Fate of microtubule-organizing centers during myogenesis in vitro. *J. Cell Biol.* 100:35–46.

Trelstad, R. L. 1970. The Golgi apparatus in chick corneal epithelium: changes in intracellular position during development. *J. Cell Biol.* 45:34–42.

Tucker, J. B., M. J. Milner, D. A. Currie, J. A. Muir, D. A. Forrest, and M. J. Spencer. 1986. Centrosomal microtubule organizing centers and a switch in the control of protofilament number for cell surface-associated microtubules during *Drosophila* wing morphogenesis. *Eur. J. Cell Biol.* 41:279–289.

Vale, R. D. 1987. Intracellular transport using microtubule-based motors. *Annu. Rev. Cell Biol.* 3:347–378.

Verde, F., J.-C. Labbé, M. Dorée, and E. Karsenti. 1990. Regulation of microtubule dynamics by cdc2 protein kinase in cell-free extracts of *Xenopus* eggs. *Nature (Lond.).* 343:233–238.

Vigers, G. P. A., M. Coue, and J. R. McIntosh. 1988. Fluorescent microtubules break up under illumination. *J. Cell Biol.* 107:1011–1024.

Wadsworth, P., and Salmon, E. D. 1986. Analysis of the treadmilling model during metaphase of mitosis using fluorescence redistribution after photobleaching. *J. Cell Biol.* 102:1032–1038.

Wadsworth, P., and M. McGrail. 1990. Interphase microtubule dynamics are cell type-specific. *J. Cell Sci.* 95:23–32.

Wang, Y.-L., F. Lanni, P. L. McNeill, B. R. Ware, and L. D. Taylor. 1982. Mobility of cytoplasmic and membrane-associated actin in living cells. *Proc. Natl. Acad. Sci. USA.* 79:4660–4664.

Warren, G., J. Davoust, and A. Cockroft. 1984. Recycling of transferrinreceptors in A431 cell is inhibited during mitosis. *EMBO (Eur. Mol. Biol. Organ.) J.* 3:2217–2225.

Webster, D. R., and G. G. Borisy. 1989. Microtubules are acetylated in domains that turn over slowly. *J. Cell Sci.* 92:57–65.

Webster, D. R., J. Wehland, K. Weber, and G. G. Borisy. 1990. Detyrosination of alpha tubulin does not stabilize microtubules in vivo. *J. Cell Biol.* 111:113–122.

Webster, D. R., G. G. Gundersen. J. C. Bulinski, and G. G. Borisy. 1987. Differential turnover of tyrosinated and detyrosinated microtubules. *Proc. Natl. Acad. Sci. USA.* 84:9040–9044.

Wojcieszyn, J. W., R. A. Schlegel, E.-S. Wu, and K. A. Jacobson. 1981. Diffusion of injected macromolecules within the cytoplasm of living cells. *Proc. Natl. Acad. Sci. USA.* 78:4407–4410.